PHYSICAL REVIEW B VOLUME 26, NUMBER 12 15 DECEMBER 1982

Low-temperature ionization of the excited F center: Evidence for lattice tunneling

M. Georgiev
Institute of Solid State Physics, Bulgarian Academy of Sciences, Sofia 1184, Bulgaria

A. Gochev
Institute of Nuclear Research and Nuclear Energy, Bulgarian Academy of Sciences, Sofia 1184, Bulgaria

S. G. Christov
Institute of Physical Chemistry, Bulgarian Academy of Sciences, Sofia 1000, Bulgaria

A. Kyuldjiev
Institute of Nuclear Research and Nuclear Energy, Bulgarian Academy of Sciences, Sofia 1184, Bulgaria

(Received 1 December 1981)

Several possible ionization mechanisms of excited F centers (F^*) in alkali halides are discussed. A lattice tunneling model for the low-temperature F^* ionization is proposed which implies considerable rearrangement of the lattice as a condition for a radiationless electron transfer from the F^* center to a virtual polaron center in the crystal. This model rests on a configurational diagram based on experimental absorption and emission data. A recent reaction-rate theory of electron hopping in polar crystals is applied to calculate the rate constant k_{12} of the F^* ionization in the temperature range 10—160 K by the use of reasonable values of four parameters: the LO vibration frequency ν, the reorganization energy E_r of the lattice, the reaction heat Q at zero temperature, and the resonance energy V_{12} of the electron transfer. In this way good agreement between the theoretical results and the available experimental data for k_{12} is obtained. In addition, an independent estimation of the "average" resonance energy, based on a simple donor-acceptor model for the electron transfer, is found to agree very well with the values of V_{12} fitted to the experiment. The average values of the electron tunneling distance $\bar{R}_t$ and the average donor-acceptor (F-center—polaron-center) separation $\bar{R}$ derived from this model seem also to be quite reasonable. Some implications of the theory concerning the reverse process of electron transfer from a free polaron to an empty ion vacancy are also discussed.

I. INTRODUCTION

The optical excitation in the F band of an F center (electron bound to anion vacancy) in the alkali halides results, after lattice relaxation, in the formation of a short-lived relaxed excited state $\tilde{F}^*$ (RES). The $\tilde{F}^*$ lifetime τ_F has been measured for the first time in KCl by Swank and Brown using both luminescence-decay and transient-photoconductivity techniques.[1] Since then a number of lifetime experiments have been performed on virtually all the alkali halides.[2] The $\tilde{F}^*$ lifetime has been found to be temperature dependent: Generally, it falls down slowly but steadily as the temperature T is raised to about 100 K, which is then followed by a much steeper decrease at higher temperatures. This latter branch of the τ_F vs T curve has been tentatively explained in terms of the ionization of the $\tilde{F}^*$ center through transition of the electron to the conduction band (CB) in a thermally activated process. The entire temperature dependence has been dealt with by means of the equation

$$\tau_F^{-1}=\tau_R^{-1}+\tau_i^{-1}+\tau_Q^{-1}\,, \tag{1}$$

where τ_R^{-1} is the radiative deexcitation rate,

$$\tau_i^{-1}=\tau_0^{-1}\exp(-E_i/k_BT) \quad (2)$$

is the thermal ionization rate (E_i being the ionization energy, τ_0^{-1}—an effective frequency factor), and τ_Q^{-1} is the rate of any other (nonradiative) deexcitation process.

Quantities closely related to τ_F are the radiative quantum yield

$$\eta_R=\tau_F/\tau_R \quad (3)$$

and the ionization efficiency

$$\eta_i=\tau_F/\tau_i\ . \quad (4)$$

It is clear that only parallel measurements of τ_F, η_R, and η_i could provide the complete experimental information on all three $\tilde{F}^*$ decay rates mentioned above. Nevertheless, most of the work done so far has involved the first two quantities (τ_F and η_R) alone, while the ionization rate τ_i^{-1} has been assumed to be of the form (2) with $\tau_0^{-1}=\nu_i$—a classical attempt frequency of the order of 10^{12} Hz. By such measurements Stiles *et al.* showed τ_R (the radiative lifetime) to be slightly decreasing with the temperature from liquid-helium temperature (LHeT) to 100 K, while η_R remained constant (equal to 1 for KCl).[3,4] This was explained in terms of the thermal population of a $2p$-like RES, more efficient in emission than the lower-lying $2s$-like state, normally occupied at low temperatures.[5] Data on the τ_Q term (assuming a "classical" ionization rate) were reported for NaF (Ref. 6) and for KF (Ref. 7) and explained in terms of Kubo and Toyozawa's[8] tunneling process to the ground state. It was also suggested that an extra temperature dependence on τ_0 and/or E_i may arise from the thermal expansion of the lattice.[9] Recently Bosi and Nimis proposed that a low-temperature variation of τ_F could arise from the interaction with a residual concentration of empty anion vacancies frozen-in during quenching.[10]

So far, all the three experimentally accessible quantities have been measured in KCl, namely, τ_F,[1,3,4,11] η_R,[2–4,11–13] as well as η_i.[2,12,13] The ionization efficiency was obtained as half the initial quantum yield $\eta_{F\text{-}F'}$ of the F-F' conversion or was extracted from photoconductivity data. The experimental data indicate clearly that the nonradiative deexcitation is unimportant in KCl.[4] The quantity $(1/\eta_i-1)^{-1}=\tau_i^{-1}/\tau_R^{-1}$ was found to follow well the Arrhenius dependence on the absolute temperature above 100 K, yielding an $\tilde{F}^*$ thermal ionization energy of 0.16 eV,[13] in agreement with values obtained in τ_F and η_R measurements. However, the apparent harmony between the classical ionization model and experiment is increasingly violated below 100 K, there remaining a residual nonvanishing ionization efficiency at temperatures as low as LHeT. Such a residual effect is also exhibited by the temperature dependence of the F-F' photoequilibrium,[12] and could well be due to the same physical reason, the F' photoequilibrium density being proportional to the square root of η_i at low conversion magnitudes. An additional indication of the low-temperature ionizability of the $\tilde{F}^*$ center comes from measurements of the photoconductivity in the F band. Although the observed low-temperature photocurrent had once been attributed to unspecified colloids,[14] it has remained basically unexplained.[15]

It should be pointed out that the observed low-temperature ionization yields, when measured as F-F' half-yields,[12] do not seem to result from any F' centers produced through electron tunneling between close F-center pairs[16,17] for the following reasons: (i) the high-temperature ultimate η_i value is unity with reasonable accuracy; (ii) the F-center system studied is fairly dilute ($\lesssim 6\times 10^{16}/\text{cm}^3$ in additively colored crystals); (iii) any tunnel-produced F' centers would contribute negligibly to the F' density measured in a steady-state—absorption experiment, since they are short lived due to the reverse tunneling process. It seems safe to conclude that the residual η_i value represents a real although greatly puzzling phenomenon of an $\tilde{F}^*$ ionization capability at unexpectedly low temperatures.[2] The low-temperature trend is also displayed by the photoequilibrium F-F' conversion versus temperature plot in KF below 100 K.[18]

Several mechanisms have been considered in the literature that must be taken into account while discussing the $\tilde{F}^*$ absorption ionizability:

(i) $\tilde{F}^*$ absorption of ir light quanta originating from the intrinsic emission due to the transverse-optical (TO) vibrations of the lattice.[19] The computed η_i vs T dependence falls well beneath the experimental points below 90 K. The agreement between theory and experiment[13] is generally poor.

(ii) Phonon-assisted transition of the F^* electron to an excited polaron band of $2p$ symmetry.[20] The computed temperature dependence of η_i, while agreeing fairly well with the experimental curve above 120 K,[13] falls beneath it at lower temperatures.

(iii) F^* autoionization before or during relaxation if the low-lying ionization states dip below those reached on absorption of F band light.[21] Although no quantitative theory seems to have been

developed,[22] it is clear that the transition from excited to ionized F states should involve rearrangement of the equilibrium lattice configuration, which requires ionic tunneling at low temperatures. The model allows for a low-temperature F-center ionizability on phonon absorption within the high-energy portion of the F band.

(iv) $\widetilde{F}^*$ ionization due to reabsorption of intrinsic $\widetilde{F}^*$ emission light quanta. The mechanism would work because of the expected overlap of the $\widetilde{F}^*$ emission and (ionization) absorption bands, as found in KI.[23,24]

(v) $\widetilde{F}^*$ ionization through $\widetilde{F}^*$-$\widetilde{F}^*$ interaction due to Auger's effect,[25] or to resonant energy transfer.[26] The latter mechanism requires that the $\widetilde{F}^*$ absorption and emission bands should overlap. Inasmuch as such an overlap has actually been found in KI, the resonant energy transfer model was used to interpret experimental data on the decay of the $\widetilde{F}^*$ population following laser pumping in the F band of that material.[23,27] Both mechanisms are dependent on the separation between $\widetilde{F}^*$ pairs and would therefore require considerable $\widetilde{F}^*$ densities. For example, the resonant energy transfer occurs as an $\widetilde{F}^*$ decay mode in KI when more than 10^{16} F centers per cm^3 are excited simultaneously. However, such very high excitation levels are not achieved by means of usual light sources.

(vi) Another possibility that has not yet been discussed relative to the F^* center is the low-temperature $\widetilde{F}^*$ ionization through lattice tunneling to low-lying ionization states in an endo- or exothermic process.[28–30] In either case such a process would require considerable rearrangement of the lattice as one goes from the RES to the equilibrium ionized states.

In what follows we shall present both experimental and theoretical arguments to justify an attempt of explaining the observed low-temperature F^* ionizability in terms of (vi). While a quantitative description will be sought of the total $\widetilde{F}^*$ ionization rate by means of a lattice-tunneling process alone, credit must also be given to other mechanisms mentioned that can also contribute to the measured ionizability. In this sense the computed effect should be considered an upper limit to the eventual contribution of tunneling.

II. CONFIGURATIONAL COORDINATE DIAGRAM FOR THE F CENTER

In its simplest form the configurational coordinate (CC) method plots the adiabatic energy of the coupled electron-phonon F-center system versus some appropriate coordinate of the ionic motion, e.g., that of the "breathing mode" around the vacancy.[31] CC diagrams were widely used earlier for describing the optical properties of defect centers in ionic crystals,[12,22,32,33] although the method involves a number of approximations.[31] The CC diagram of the F center in KCl is presented in Fig. 1 exhibiting the parabolas for the ground electron state F_0, the first excited state F^*, and the low-lying ionized state F^+. Both F^* and F^+ are assumed to be single-electron states and the complications arising from the mixture of states of different parity will be ignored. In computing the CC diagrams for F_0 and F^* we used the method of Lüty and Gebhardt,[34] taking into account the more accurate absorption and emission data of Gebhardt and Kuhnert.[35] This necessitated introducing slight corrections in only the F^* curve. The F^+ parabola was obtained using the longitudinal-optic (LO) phonon frequency[31] $\omega_{LO}=4.02\times10^{13}$ Hz and the effective mass of the LO oscillator $M_{LO}=M_K M_{Cl}/(M_K+M_{Cl})$ to compute the force constant $f_i=M_{LO}\omega_{LO}^2=3.12$ eV/Å^2. The approximate horizontal and vertical positions of the F^+

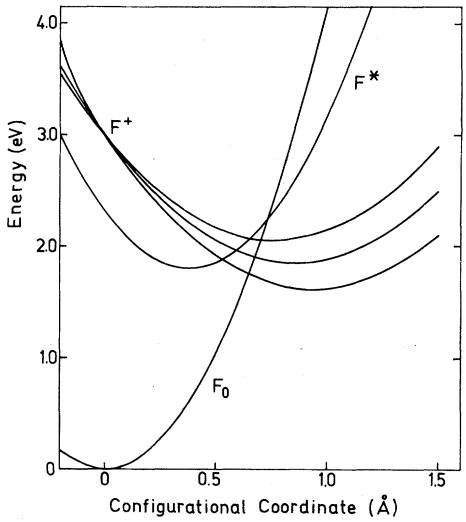

FIG. 1. Configurational coordinate diagram of the KCl F center. F^* and F_0 label the potential energy curves for the first excited and ground electron states, respectively, F^+ denotes three potential energy curves for the ionization state, computed at three different values of the relaxed—excited-state optical ionization energy (0.3, 0.4, and 0.5 eV), and at the same threshold energy for optical ionization of the ground state (3 eV).

curve were calculated using the direct optical-ionization threshold energies of $\tilde{F}_0$ and $\tilde{F}^*$. The former was determined to be about 3 eV from the spectral photoconductivity data of Wild and Brown.[36] The latter was never measured in KCl; however, in KI it is about 0.3 eV.[24] The ratio of the $\tilde{F}^*$ thermal ionization energies in KCl and KI is 0.15:0.11=1.36.[31] Using the relation between optical and thermal ionization energies of a Coulomb center,[37] we corrected the above-mentioned ratio for the dielectric constants (optical and static) of KCl and KI to obtain 0.49 eV for the $\tilde{F}^*$ optical ionization energy in KCl. In fact, this is just a rough estimate, because the F^* electronic state is only approximately hydrogenlike. Accordingly, we present in Fig. 1 three F^+ parabolas computed at three different values for the $\tilde{F}^*$ optical ionization energy: 0.3, 0.4, and 0.5 eV.

Two general features are displayed by the CC diagram in Fig. 1. First, there seems to be considerable lattice relaxation following the change of the electronic state from $\tilde{F}^*$ to $\tilde{F}^+$. Second, the possibility is not excluded that the minimum of F^+ may be nearly equal or even lie lower than that of F^*. In any case, the transition from $\tilde{F}^*$ to $\tilde{F}^+$ would require overcoming a barrier of the order of some tenths of an eV through classical or quantum motion of the ions coupled to the F-center electron, depending on the temperature. For the exothermic direction of the process ($\tilde{F}^+$ lower than $\tilde{F}^*$) the F^* ionization could proceed even at the lowest temperatures via lattice tunneling through the barrier. In the endothermic case ($\tilde{F}^+$ higher than $\tilde{F}^*$) the low-temperature ionizability of $\tilde{F}^*$ will be negligible, though there could be considerable deviation from the Arrhenius law as a result of the lattice tunneling before a real classical behavior is established at higher temperatures.

In the following sections we shall discuss on the basis of CC diagrams of Fig. 1 the reaction rates for both the exothermic and endothermic situations and compare them with the experiment.

III. THEORETICAL MODEL

A general theory of reaction rates in both gas and condensed phases has been developed[28–30,38,39] in which both the electron and nuclear motions are treated quantum mechanically within the framework of the Born-Oppenheimer (adiabatic) approximation. The theory avoids the restrictions of the classical (semiclassical) theories and those of the quantum-mechanical perturbation theory. It leads to the following general expression for the rate constant:

$$k_{1,2}=\kappa(k_BT/h)(Z^*/Z)\exp(-E_c/k_BT)\ . \quad (5)$$

Here E_c is the "classical activation energy" for the endothermic direction of reaction (Fig. 2), Z is the complete partition function of reactants, and Z^* is the partition function of their nonreactive modes. The factor $\kappa \gtrless 1$ is the exact quantum correction to the classical (semiclassical) rate constant, defined in terms of the total transition probability averaged over the quantum states of the nonreactive modes of the reactants. The rate constant for the reverse exothermic reaction direction is

$$k_{2,1}=k_{1,2}\exp(Q/k_BT)\ \ (Q>0)\ , \quad (6)$$

where $Q>0$ is the reaction heat at 0 K, the classical activation energy now being E_c-Q. For more details on the general formulation of the theory the reader is referred to the quoted papers.[38,39]

We shall apply the above-mentioned reaction-rate theory to a simple model of the crystal considered as a system of harmonic oscillators with the same frequency ν in both the initial and final electron states. The adiabatic potential energy of the system in both states is then described by two similar many-dimensional rotational paraboloids, which intersect along a line representing a transition-state configuration of the crystal lattice. Because of the electronic coupling between the two localized electronic states a "resonance" splitting in the intersection region results in the formation of a lower and an upper adiabatic surface. The "reaction coordinate" x is a straight line connecting the positions of the minima of the two paraboloids. This coordinate is dynamically separable from the other coordinates of the crystal lattice. This fact greatly simplifies the calculation of the transition probability, which thus reduces to a one-dimensional problem. A cross cut along x is illustrated in Fig. 2, which corresponds to the CC diagrams in Fig. 1. Similar diagrams were considered by Seitz and by Mott and Gurney when they discussed the luminescent properties of defect centers.[37]

The coupled electron-lattice system can perform transitions from the initial to the final state described in the lattice configuration space by the motion along the reaction coordinate x. In principle, both classical (over-barrier) and quantum-mechanical (tunneling) transitions of the lattice, which must overcome the potential barrier on the lower adiabatic surface, are possible.

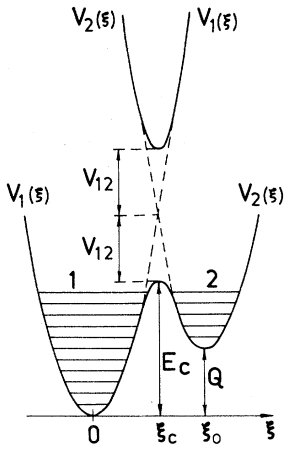

FIG. 2. Cross cut along the reaction coordinate of a potential energy surface resulting from the intersection of two rotational paraboloids representing the electronic energies of reactants and products, respectively. [$\xi=2\pi(M\nu/h)^{1/2}x$ is a dimensionless coordinate used in place of the Cartesian coordinate x.] $V_1(\xi)$ and $V_2(\xi)$ are the corresponding energy profiles for the initial and final states of the system. V_{12} is the resonance energy at the crossing point ($\xi=\xi_c$) of the potential curves $V_1(\xi)$ and $V_2(\xi)$, Q is the reaction heat at 0 K, and E_c is the classical activation energy for the endothermic reaction direction.

The simple model described above is completely solved mathematically,[29,38] in particular, in the low-temperature range of strong lattice tunneling $T<T_c/2$, where T_c is Christov's characteristic temperature.[28,38] In this range the rate expression (5) turns into

$$k_{1,2}=\nu\exp(h\nu/2k_BT)\times\sum_{n_1}W_l(E_{n_1})W_e(E_{n_1})\exp(-E_{n_1}/k_BT)\ . \quad (7)$$

Here, W_l is the probability of the lattice tunneling given by[29,38,39]

$$W_l(E_{n_1})=\frac{\pi F^2(\xi_0,\xi_c)}{2^{n_1+n_2}n_1!n_2!}\times e^{-(n_1-n_2)^2h\nu/E_r}e^{-E_r/h\nu}\ , \quad (8)$$

where

$$F(\xi_0,\xi_c)=\xi_0H_{n_1}(\xi_c)H_{n_2}(\xi_c-\xi_0)-2n_1H_{n_1-1}(\xi_c)H_{n_2-1}(\xi_c-\xi_0)+2n_2H_{n_1}(\xi_c)H_{n_2-1}(\xi_c-\xi_0) \quad (8')$$

contains Hermitian polynomials of order n_1, n_2, n_1-1, and n_2-1, $\xi=2\pi(M\nu/h)^{1/2}x$ is a dimensionless and x a Cartesian vibrational coordinate, and M is the effective mass of the lattice vibrations, assumed to be the same in both electronic states. The subscripts o and c refer to the positions of the crossing point (ξ_c) of the parabolic potentials V_1 and V_2 (Fig. 2) and the minimum of V_2 (ξ_0), the minimum of V_1 being at $\xi=0$. In (8)

$$E_n=(n+\tfrac{1}{2})h\nu \quad (8'')$$

is the vibrational energy, and n_1 and n_2 are the quantum numbers of the initial and final states, while

$$E_r=h\nu\xi_0^2/2=fx_0^2/2 \quad (8''')$$

is the so-called "reorganization energy" of the oscillator system, where f is the force constant of the vibration.

In (7) W_e is the electron transition probability[30,38,39]

$$W_e(E_n)=\frac{2\pi}{\gamma_n\Gamma^2(\gamma_n)}e^{-2\gamma_n(1-\ln\gamma_n)}\ , \quad (9)$$

where

$$\gamma_n=(V_{12}^2/2h\nu)[1/E_r(E_c+V_{12}-E_n)]^{1/2}\ , \quad (9')$$

while V_{12} is the resonance energy that is a measure of the two-site electron interaction. Γ is the gamma function.

The adopted model introduces four parameters: ν, E_r, Q, and V_{12}. The barrier height E_b is related to E_r, Q, and V_{12} by[29,38,39]

$$E_b=E_c=\frac{(E_r+Q)^2}{4E_r}-V_{12}\ \text{(endothermic)}\ ,\qquad E_b=E_c-Q=\frac{(E_r-Q)^2}{4E_r}-V_{12}\ \text{(exothermic)}\ . \quad (10)$$

All these parameters can be obtained, in principle, from a detailed F-center theory.

We assume that the F^* ionization occurs by electron tunneling from a donor state (F^*) to an acceptor state (F^+), which is a virtual-polaron state. The electron tunneling is made possible through lattice reorganization from the initial configuration $\xi=0$ to the transition configuration corresponding to the crossing point $\xi=\xi_c$ of the "diabatic" curves V_1 and V_2 at which the electronic energies of states 1 and 2 are equal. A constant donor-acceptor separation during the electron transfer is assumed. This means that the subse-

quent translational motion of the polaron relative to the ionized donor (F^+) center is neglected in calculating the electron transition probability, which implies that this motion is slow when compared to the lattice vibrations.[40] The lattice reorganization leading to the appropriate transition configuration, which is necessary for the electron transfer to occur, is controlled by the ionic vibrations in both the polaron state and in the neighborhood of the F^* center. The former are in fact LO vibrations while the latter may be different; however, we assume that their frequency ν is close to ν_{LO} and is higher than that related to the $F^* \rightarrow F_0$ radiative transition ($\nu_e < \nu \lesssim \nu_{LO}$). Insofar as the above assumption is justified, the single-frequency and single-reduced-mass oscillator model adopted here may be expected to be a fair approximation to reality.

IV. APPLICATION OF THE MODEL TO THE KCl EXCITED F-CENTER IONIZATION

Data on the $\tilde{F}^*$ ionization rate $\tau_i^{-1} = \eta_i / \tau_F$ in KCl computed from the experimental data on[2,12,13] η_i and on[1-4,11] τ_F are plotted in Fig. 3 by corresponding data points versus the respective absolute temperature between 10–160 K. In addition, results of similar calculations by Stiles *et al.*[4] based on their data of η_R and τ_F under the assumption that τ_Q^{-1} is negligible (giving $\eta_i = 1 - \eta_R$) are also shown. The agreement between these and the remaining points, based on the direct experimental measurements of η_i, lends support to Stiles's assumption. It is seen that while data from different sources agree fairly well above 100 K, there is considerable difference at lower temperatures between points obtained using F-F' measurements[12,13] and photoconductivity data.[2] Nevertheless, both sets of low-temperature data point to (i) a considerable deviation from the Arrhenius law and (ii) the existence of a residual F^* ionizability, those obtained from $\eta_{F\text{-}F'}$ lying some 2 orders of magnitude higher than those calculated from the F photocurrent.

A further attempt was made to process the data in Fig. 3 in terms of the lattice-tunneling model of Sec. III. Three types of reactions were tried; exothermic ($Q < 0$), isothermic ($Q = 0$), and endothermic ($Q > 0$). Best fits were obtained assuming the LO-oscillator frequencies ($\omega_{LO} = 4.02 \times 10^{13}$ Hz for KCl), while the remaining parameters were varied.

Three representative examples are shown in Fig. 3 by solid lines labeled a, $Q = 0$; b, $Q = -h\nu$; c, $Q = h\nu$. Curve c (endothermic) agrees well with the experimental data down to 70 K but does not at all explain the low-temperature ionization below that temperature. One concludes that either the process is not endothermic, or that there exists some other process in addition to c that is only weakly or not temperature dependent and is responsible for the residual ionization. Curves a (isothermic) and b (exothermic) both describe well the experimental situation within the whole temperature range studied, except for a small range between 60 and 90 K. This description does not apply to the F-F' point below 100 K.

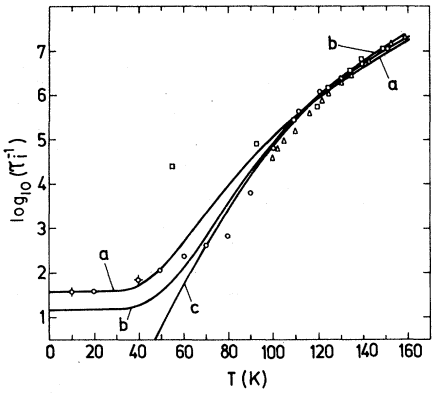

FIG. 3. Temperature dependence of the ionization rate $k_i = \tau_i^{-1}$ of the F^* center. The theoretical curves are calculated by Eqs. (6), (7), (8), and (9) with the following parameter values: $\omega = \omega_{LO} = 4.02 \times 10^{13}$ Hz. Curve a (isothermic, $Q = 0$): $V_{12} = 0.01$ eV, $E_r = 0.7282$ eV. Curve b (exothermic, $Q = -h\nu_{LO}$): $V_{12} = 0.03$ eV, $E_r = 0.9000$ eV. Curve c (endothermic, $Q = h\nu_{LO}$): $V_{12} = 0.02$ eV, $E_r = 0.7541$ eV. The experimental points are □, Swank and Brown, Ref. 1 (τ_F) and Luty, Ref. 12 (η_i); △, Stiles *et al.* Ref. 4 (τ_i^{-1}) 0, Stiles *et al.* Ref. 4 (τ_F) and Bosi *et al.* Ref. 2 (η_i); +, Bosi *et al.* Ref. 2, (τ, η_i).

V. DISCUSSION OF THE RESULTS

Our calculations are essentially based on the CC diagrams of type shown in Fig. 1, which cannot be easily understood within the framework of the large-orbit model of the $\tilde{F}^*$ center.[31] One of the implications of this model is that there will be very little lattice relaxation as the electron state changes from $\tilde{F}^*$ to $\tilde{F}^+$ because of the assumed diffuse character of the $\tilde{F}^*$ electron wave function,[41] in contrast to the situation depicted by the F^+ curves

in Fig. 1. This situation is, however, consistent with some experimental indications of a more compact RES in KI.[42] In such a case, a great deal of lattice relaxation could be expected as one goes from $\tilde{F}^*$ to $\tilde{F}^+$. It is to be stressed that the F^+ curves were computed using experimental data of the optical ionization energies of $\tilde{F}_0$ and $\tilde{F}^*$ that are characteristic of the direct vertical transitions, according to the Franck-Condon principle. All three of these curves display the large relaxation behavior, contrary to earlier calculations.[43,44] Assuming a relative invariance of E_r, it may also be expected that according to (8''') the magnitude of the displacement $x_0=(2E_r/f)^{1/2}$ between the equilibrium positions of F^+ and F^* will increase in the order LiF-NaF-KF-RbF-NaCl-LiCl-KCl-RbCl-NaBr-KBr-RbBr-NaI-KI-RbI due to the decrease of the LO force constant f in the same order. Therefore, the lattice-tunneling ionization effect may eventually be more pronounced in the iodides and the bromides than it is in the chlorides and the fluorides. The effect may even be completely absent in NaF where a low-magnitude crossover barrier between F^* and F_0 (Ref. 45) apparently favors a strong τ_Q term, presumably by means of the Kubo-Toyozawa tunneling deexcitation process.[6]

The fair agreement between curves *a* and *b* on one hand and the experimental points on the other, as shown in Fig. 3, suggests $\tilde{F}^*$ ionization through an isothermic or an exothermic lattice tunneling channel releasing little reaction heat ($Q\sim h\nu_{\mathrm{LO}}$). This conclusion depends critically on the existence of the low-temperature τ_i^{-1} points below 60 K. However, as mentioned in Sec. I, a residual $\tilde{F}^*$ ionizability could arise, in principle, due to a variety of mechanisms. A residual temperature-independent term $k_0=40\ \mathrm{s}^{-1}$ if added to the endothermic rate constant (Fig. 3, curve *c*) would also lead to a similar fair agreement with experiment, as that displayed by the isothermic and exothermic curves *a* and *b* in Fig. 3. Therefore, an unambiguous determination of the actual mechanisms of F^* ionization at low temperatures ($T<60$ K) is necessary. Moreover, assuming the validity of the lattice tunneling model one needs an independent estimation of the fitting parameters in order to check the above three possibilities ($Q=0$, $Q>0$, and $Q<0$). In any event there seems to be little doubt in that the observed low-temperature deviations from the Arrhenius law[2] arise from lattice tunneling.

Our calculations show that ν_{LO} is an appropriate parameter in the adopted one-frequency oscillator model for the $\tilde{F}^*$ ionization. This is in agreement with the polaron theories[46] that assume that the electron is most strongly coupled to the nonlocalized LO modes of the crystal lattice.

The best fit for the reorganization energy $E_r=0.73$ eV is some 50% higher than the one computed from KI data for the optical ionization energy of F^* which is closely related to E_r. Nevertheless, this seems to be a reasonable value, being of the expected order of magnitude for KCl. With the use of the value $E_r=0.73$ eV from (8''') the separation between the equilibrium positions of F^* and F^+ is found to be $x_0=0.68$ Å.

The best adjusted values of the resonance energy $V_{12}=0.01-0.03$ eV should be considered as effective ones, since the electron transfer actually does not occur between two fixed centers, as presumed in the physical model, but rather from a fixed donor (F^*) to a virtual acceptor (polaron) situated on a sphere with an effective radius R_{eff}.

Nevertheless, an independent theoretical estimation, based on a simple one-dimensional two-site tunneling model for the electron transfer, yields "average" values for V_{12} that agree surprisingly well with those found from the fitting to experiment. The details of these calculations are given in the Appendix. There it is shown that the above values of V_{12} (0.01−0.03 eV) correspond to an average tunneling distance $\bar{R}_t$ within the range 10−25 Å and an average donor-acceptor separation $\bar{R}$ that varies from 55 to 180 Å. These estimates for $\bar{R}_t$ and $\bar{R}$ seem to be quite reasonable from the physical point of view.

From the above-mentioned calculations it is seen that the F^* electron in KCl should tunnel over a mean distance that is somewhat larger than two lattice spacings (2×6.294 Å$=12.588$ Å) to become bound into a polaron state. The center of the polaron is about 12 lattice spacings apart from the ion vacancy, but even at such a large distance the electron motion may be considerably affected by the vacancy.

With the parameter values given in Fig. 3 the electron transition probability W_e, as calculated by Eq. (9), is found to be $W_e=0.03-0.3$, which corresponds to the intermediate range between the limits $W_e=1$ and $W_e\ll 1$ of adiabatic and nonadiabatic transitions.

Using the values $V_{12}=0.019$ eV and $E_r=0.73$, 0.75, and 0.90 eV in Eq. (10) the barrier height for lattice reorganization is found to be $E_b=0.16$ eV ($Q=0$), $E_b=0.18$ eV ($Q=-h\nu$), and $E_b=0.19$ eV ($Q=h\nu$). In all three cases the transition of the electron-lattice system in the temperature range

100–150 K occurs with the highest probability from the fifth vibrational level $n_1=5$ or $n_2=5$ ($Q=-h\nu$) of the initial state, which corresponds to an apparent activation energy $E_a=0.15$ eV, in excellent agreement with that obtained from the Arrhenius τ_i^{-1} vs $1/T$ plot for KCl.

As discussed above, no choice between the three possibilities $Q=0$, $Q>0$, and $Q<0$ is possible for the time being because of the lack of any sufficient experimental information. Despite this fact it may be concluded that the lattice-tunneling theory provides a reasonable explanation of the available experimental data on the $\tilde{F}^*$-center ionization in the low-temperature range.

An important question arises as to the temperature dependence of the process that is the reverse of the F^* ionization. The trapping coefficient γ_α of a free polaron by an empty anion vacancy has been discussed by Pekar.[47] One of the implications of the present model is that the rate at which a polaron having already met the vacancy should go into a bound F^* state will be determined by $k_{1,2}(T)$ if the F^* ionization is described by $k_{2,1}(T)$, and *vice versa*. Accordingly, the temperature dependence of the binding rate will be given by one of the curves in Fig. 3. In particular, there will be a residual binding rate at the lowest temperatures if $Q\gtrsim 0$. At not too low a temperature the binding rate will be high, and the overall trapping coefficient will be determined by the probability of polaron collision with the vacancy. However, as the temperature is lowered the binding probability will gradually decrease, and binding may become the rate-determining process. Such a trend seems to be displayed by the γ_α vs T plot[48] for KBr below 50 K down to 24 K, where a deviation from the collision coefficient is observed in the direction predicted by the lattice-tunneling theory. Clearly, more experimental data are needed before any definite conclusions are reached that may turn out to be crucial in checking the validity of the present model.

APPENDIX: ESTIMATION OF THE RESONANCE ENERGY V_{12}

Assuming a symmetric one-dimensional double well (Fig. 4) to describe the electron potential energy in a donor-acceptor (DA) pair at a separation R, the quasiclassical expression for the resonance energy is[49]

$$V_{12}=\frac{\hbar\omega_e(R)}{\pi}e^{-\alpha(R)}\,,$$
$$\alpha(R)=(2m/\hbar^2)^{1/2}\int_{a_1}^{a_2}[U(r,R)-E_e]^{1/2}dr\,, \tag{A1}$$

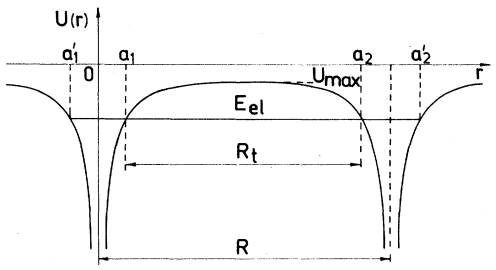

FIG. 4. One-dimensional diagram for electron tunneling between two symmetric potential wells, at a fixed DA-pair separation R. r—electron coordinate; $U(r)$—electron potential energy; $U_{\max}$—maximum of the potential barrier; E_e—total electron energy; a_1,a_2,a_1',a_2'—classical turning points; $R_t=a_2-a_1$—tunneling distance.

where

$$\omega_e(R)=\pi/\theta_e(R),$$
$$\theta_e(R)=(2m)^{1/2}\int_{a_1'}^{a_1}[E_e-U(r)]^{-1/2}dr\,. \tag{A1'}$$

ω_e is the frequency of the electron motion within the potential well 1 or 2, E_e is the total electron energy, r is the electron coordinate, a_1 and a_1' are the classical turning points in well 1, while a_2 and a_2' are those in well 2, and m is the (effective) electron mass. Note that generally both α and ω_e depend on R.

In Fig. 4 $U(r)$ represents the electron potential energy at a fixed lattice configuration corresponding to the transition state $x=x_c$ ($\xi=\xi_c$) in the CC diagram (Fig. 2) at which the total electron energies in wells 1 and 2 are the same. It can be expected that a Coulomb double well will be a good approximation to the electron potential energy of a F^*-polaron DA pair as long as not only the polaron but also the $\tilde{F}^*$ electron potential is largely Coulomb above the RES energy level, as assumed in the semicontinuous approach to the F center.[31] However, at the transition lattice configuration ($x=x_c$) both potentials differ from the corresponding ones at the equilibrium lattice configurations ($x=0$ and $x=x_0$).

The actual potential distribution about the DA pair has an axial space symmetry; however, the electron tunneling occurs with the highest probability along the symmetry axis, i.e., the line r connecting the DA pair. Consequently, in an approximate treatment, the three-dimensional tunneling problem can be reduced to a one-dimensional problem.

The electron potential energy in a symmetric Coulomb double well is given by

$$U(r)=-(e^2/\epsilon)R/r(R-r) \quad (0<r<R), \tag{A2}$$

where ϵ is the dielectric constant of the crystal. This expression takes into account the influence of well 2 on the electron motion in well 1 and *vice versa*. $U(r)$ has a maximum

$$U_{\max}=4E_e(\rho/R), \quad \rho=-e^2/\epsilon E_e \tag{A3}$$

at $r=R/2$. The electron transition from well 1 to well 2 will occur by tunneling if $E_e<U_{\max}$, which corresponds to $R>4\rho$. Under this condition the classical turning points a_1 and a_2 are defined by

$$a_{1,2}=\tfrac{1}{2}R[1\mp(1-4\rho/R)]^{1/2} \tag{A4}$$

so that the exponent $\alpha(R)$ in (A1) becomes

$$\alpha(R)=(2m/\hbar^2)^{1/2}\int_{a_1}^{a_2}[U(r)-E_e]^{1/2}dr$$

$$=c\int_{a_1}^{a_2}[(r-a_1)(a_2-r)/r(R-r)]^{1/2}dr$$

or making the substitution $s=r-\frac{1}{2}R$

$$\alpha(R)=2c\int_0^{R_t/2}\frac{s^2-(\frac{1}{2}R_t)^2}{[s^2-(\frac{1}{2}R)^2]^{1/2}}ds \tag{A5}$$

where

$$c=(-2mE_e/\hbar^2)^{1/2} \tag{A6}$$

and

$$R_t=a_2-a_1=R[1-(4\rho/R)]^{1/2}$$

is the tunneling distance.

The integral in (A5) can be evaluated by a transformation, giving

$$\alpha(R)=c[RE(k)-4\rho K(k)]$$

$$=4c\rho\left[\frac{E(k)}{1-k^2}-K(k)\right], \tag{A7}$$

where $K(k)$ and $E(k)$ are the complete elliptic integrals of first and second kind, respectively, with a modulus

$$k=R_t/R=[1-(4\rho/R)]^{1/2}, \tag{A7'}$$

which represents the tunneling distance in units of the DA-pair separation R.

If the influence of well 2 on the electron motion in well 1 and *vice versa* is neglected, then in lieu of Eq. (A2) the electron potential energy will be represented by

$$U(r)\equiv U_1(r)=-(e^2/\epsilon)/r \quad (r<R/2)$$
$$U(r)\equiv U_2(r)=-(e^2/\epsilon)/(R-r) \quad (r>R/2)\,. \tag{A8}$$

Then $U(r)$ has a maximum value at $r=\frac{1}{2}R$ given by

$$U_m=2E_e(\rho/R), \quad \rho=-e^2/\epsilon E_e\,. \tag{A9}$$

An evaluation of the exponent $\alpha(R)$ in (A1) with the potential (A8) is possible by numerical integration.

The actual situation in a DA pair in which the donor is an excited F center and the acceptor is a polaron corresponds to an *asymmetric* electron potential that has an intermediate course between the symmetric potentials (A2) and (A8). Indeed, if the electron is initially in the F center (well 1), its potential energy is described by the undisturbed Coulomb potential $U_1(r)$, while after the electron transfer to the polaron center and the creation of well 2 the corresponding Coulomb potential $U_2(r)$ is perturbed by the ion vacancy (well 1). However, in a steady state, in which a rapid electron oscillation between the two wells occurs, a perturbation of well 1 (F^* state) due to the existence of well 2 (polaron state) will lead to a self-consistent potential that conserves the initial asymmetry. This is because well 1 is influenced only by the polarization around the polaron center while well 2 is affected by both the ion vacancy and the polarization around the F center. In any case, the real electron potential of the F^*-polaron DA pair at $x=x_c$ will be an intermediate one between the potentials (A2) and (A8). Therefore, calculations with these potentials will give a lower and an upper limit of the exponent $\alpha(R)$ in (A1) and the tunneling distance $R_t=a_2-a_1$.

The preexponential factor in (A1) can be evaluated in a closed form by (A1') for an isolated Coulomb center, i.e., for the situation in which the electron motion in the excited F center is governed by the unperturbed potential $U_1(r)$ in Eq. (A8), hence ω_e is independent of the DA separation R. Then one obtains

$$\theta_e=(2m)^{1/2}\left[\int_{-\rho}^{0}\left[E_e-\frac{e^2}{\epsilon r}\right]^{-1/2}dr+\int_0^{\rho}\left[E_e+\frac{e^2}{\epsilon r}\right]^{-1/2}dr\right], \tag{A10}$$

where ρ is defined by (A3), or introducing $t=r/\rho$

$$\theta_e = 2\beta\rho \int_0^1 \left[\frac{t}{1-t}\right]^{1/2} dt = \pi\beta\rho \,, \tag{A11}$$

where $\beta=(-2m/E_e)^{1/2}$. From (A1') and (A11)

$$\omega_e = \pi/\theta_e = 1/\beta\rho = (\epsilon E_e/2me^2)^{3/2} \,. \tag{A12}$$

For the double-well potential (A2) ω_e can be estimated on the basis of (A1') by numerical integration. It should be noted that the value of ω_e is only slightly dependent on the potential form and the electron energy.

The total electron energy E_e^0 of an isolated F center can be computed from the formula

$$E_e^0 = -me^4/2\hbar^2\epsilon^2 n^2 \tag{A13}$$

for the hydrogen-atom model of the F center[37] (with $n=2$ for the first excited state F^*). This formula implies a static polarization corresponding to the equilibrium lattice configuration ($x=0$). However, in the transition configuration ($x=x_c$) E_e is increased by an amount $E_c'=E_c+V_{12}$ where E_c is given by Eq. (10). On the other hand, the deformation of the F^*-potential well due to the influence of the polaron center leads to a decrease of E_e however, the extent of compensation of both effects is difficult to estimate. In any case, $E_e^0+E_c'$ is obviously an upper limit for the electron energy E_e, while $E_e^0+U_{\max}(E_e^0)$, with $U_{\max}$ given by Eq. (A3) for $E_e=E_e^0$ is a lower limit for E_e.

Inserting the values[31] $\epsilon=\epsilon_\infty=2.19$, $m=0.5m_e$, $n=2$ in Eq. (A13) one obtains $E_e^0=-0.35$ eV, and from Eq. (13) the corresponding value for $U_{\max}$ is found to be -0.335 eV. For $E_c'\simeq E_c$ use can be made of the estimates based on the fitting parameters (E_r,Q), which yields $E_c'=0.18-0.20$ eV. Thus we conclude that E_e is within the range between -0.15 and -0.70 eV. Therefore calculations were performed for three energy values in this range: -0.15, -0.35, and -0.50 eV.

The electron tunneling distance R_t depends strongly on the DA-pair separation R. With decreasing R both the maximum $U_{\max}$ of the electron potential (A2) and the energy level E_e in the potential wells decrease. A lower limit of the average value $\bar{R}_t$ of R_t can be found if only the R dependence of $U_{\max}$ given by Eq. (A3) is taken into account at a constant value $E_e=E_e^\infty$ corresponding to infinite DA separation ($R=\infty$). Indeed, the actual electron energy level at any finite value of R is lower than E_e, hence the actual tunneling distance is larger than that at E_e. Since $E_e^\infty=U_{\max}$ or $R_t=0$ at $R=4\rho$ [see Eq. (A6)], the lower limit of $\bar{R}_t$ is defined by

$$\bar{R}_t = \frac{\int_{4\rho}^{\infty} R_t(R)P_t(R)dR}{\int_{4\rho}^{\infty} P_t(R)dR} \,, \tag{A14}$$

where $R_t(R)$ is given by Eq. (A6) and $P_t(R)$ is the tunneling probability for which the quasiclassical WKB expression

$$P_t(R) = e^{-2\alpha(R)} \tag{A15}$$

may be used with $\alpha(R)$ given by (A5). From Eqs. (A14) and (A15) one obtains

$$\bar{R}_t = 4\rho \frac{\int_0^1 \frac{\exp[-2\alpha(k)]k^2 dk}{(1-k^2)^3}}{\int_0^1 \frac{\exp[-2\alpha(k)]k}{(1-k^2)^2} dk} \,, \tag{A16}$$

where the integration variable R is replaced by k by means of Eq. (A7'). The integrals in (A16) can be evaluated numerically.

From (A6) the average DA-pair separation is found to be

$$\bar{R} = 2\rho \left\{1+\left[1+\left[\frac{\bar{R}_t}{2\rho}\right]^2\right]^{1/2}\right\} \,, \tag{A17}$$

where $\bar{R}_t$ is given by (A16). Inserting the value of $\bar{R}$ in Eq. (A1), one finds $\alpha(\bar{R})$, and using Eq. (A12) for ω_e, one obtains an "average" value $V_{12}(\bar{R})$ of the resonance energy for a fixed electron energy E_e.

All approximations involved in the above treatment give a lower limit for the values of $\bar{R}_t$ and $\bar{R}$, which corresponds to an upper limit for the value of $V_{12}(\bar{R})$. The numerical results of our calculations are presented in Table I. It is seen that a variation of the electron energy E_e in the wide range considered between -0.15 and -0.50 eV does not affect the order of magnitude of the average tunneling distance $\bar{R}_t$ and the "average" resonance energy $V_{12}(\bar{R})$. It is very satisfying that the values of $V_{12}(\bar{R})$ thus calculated agree well with the fitting values given in the text, which range between 0.01 and 0.03 eV. The corresponding values for $\bar{R}_t$ and $\bar{R}$ seem also to be quite reasonable.

TABLE I. Electron tunneling parameters: E_e, total electron energy; ω_e electron frequency; $\bar{R}_t$, average tunneling distance, $\bar{R}$, average DA separation; $V_{12}(\bar{R})$, "average" resonance energy.

E_e (eV)	ω_e	$\bar{R}_t$ (Å)	$\bar{R}$ (Å)	$V_{12}(\bar{R})$ (eV)
-0.150	4.1×10^{14}	25	179	0.005
-0.350	2.7×10^{14}	14	78	0.019
-0.500	2.2×10^{14}	10	54	0.032

[1]R. K. Swank and F. C. Brown, Phys. Rev. Lett. 8, 10 (1962).
[2]L. Bosi, P. Podini, and G. Spinolo, Phys. Rev. 175, 1133 (1968).
[3]L. F. Stiles, M. P. Fontana, and D. B. Fitchen, Solid State Commun. 7, 681 (1969).
[4]L. F. Stiles, M. P. Fontana, and D. B. Fitchen, Phys. Rev. B 2, 2077 (1970).
[5]M. Tomura, T. Kitada, and S. Honda, J. Phys. Soc. Jpn. 23, 454 (1967).
[6]M. Tomura and S. Honda, J. Phys. Soc. Jpn. 26, 871 (1969).
[7]S. Honda and M. Tomura, J. Phys. Soc. Jpn. 29, 522 (1970).
[8]R. Kubo and Y. Toyozawa, Progr. Theor. Phys. 13, 160 (1955).
[9]G. Spinolo and W. B. Fowler, Phys. Rev. 138, A661 (1965).
[10]L. Bosi and M. Nimis, Phys. Status Solidi B 95, 615 (1979).
[11]R. K. Swank and F. C. Brown, Phys. Rev. 130, 34 (1963).
[12]F. Lüty, Halbleiterprobleme 6, 238 (1961).
[13]H. Fedders, M. Hunger, and F. Lüty, J. Phys. Chem. Solids 22, 299 (1961).
[14]F. Seitz, Rev. Mod. Phys. 18, 384 (1946); 26, 7 (1954).
[15]U. Haupt, Z. Phys. 176, 560 (1963).
[16]F. Porret and F. Lüty, Phys. Rev. Lett. 26, 843 (1971).
[17]Y. Ruedin, P.-A. Schnegg, C. Jaccard, and M. A. Aegerter, Phys. Status Solidi B 54, 565 (1972); 55, 215 (1973).
[18]W. C. Collins and I. Schneider, J. Phys. Chem. Solids 37, 917 (1976).
[19]H. Wille and F. Wahl, Z. Naturforsch. 21a, 304 (1966).
[20]D. Stocker, Z. Naturforsch. 23a, 1158 (1968).
[21]D. L. Dexter, C. C. Klick, and G. A. Russell, Phys. Rev. 100, 603 (1955).
[22]D. L. Dexter, Nuovo Cimento Suppl. 7, 245 (1958).
[23]K. Park, Phys. Rev. 140, A1735 (1965).
[24]K. Park and W. L. Faust, Phys. Rev. Lett. 17, 137 (1966).
[25]A. A. Berezin, Fiz. Tverd. Tela (Leningrad) 11, 1587 (1969).
[26]D. L. Dexter, J. Chem. Phys. 21, 836 (1953).
[27]D. Fröhlich and H. Mahr, Phys. Rev. 148, 868 (1966).
[28]S. G. Christov, Ber. Bunsenges. Phys. Chem. 76, 507 (1972); 78, 537 (1974).
[29]S. G. Christov, Ber. Bunsenges. Phys. Chem. 79, 357 (1975); see also J. Electrochem. Soc. 124, 69 (1977).
[30]S. G. Christov, Int. J. Quantum Chem. 16, 353 (1979).
[31]W. B. Fowler, in *Physics of Color Centers,* edited by W. Beall Fowler (Academic, New York, 1968).
[32]G. A. Russell and C. C. Klick, Phys. Rev. 101, 1473 (1956).
[33]C. C. Klick and J. H. Schulman, in *Solid State Physics,* edited by H. Ehrenreich, F. Seitz, and D. Turnbull (Academic, New York, 1957), Vol. 5, p. 97.
[34]F. Lüty and W. Gebhardt, Z. Phys. 169, 475 (1962).
[35]W. Gebhardt and H. Kühnert, Phys. Lett. 11, 15 (1964).
[36]R. L. Wild and F. C. Brown, Phys. Rev. 121, 1296 (1961).
[37]N. F. Mott and R. W. Gurney, *Electronic Processes in Ionic Crystals* (Oxford, 1948).
[38]S. G. Christov, *Collision Theory and Statistical Theory of Chemical Reactions,* Vol. 18 of *Lecture Notes in Chemistry* (Springer, Berlin, 1980).
[39]S. G. Christov, Phys. Rev. B 26, 6918 (1982).
[40]This adiabatic approximation is discussed in Ref. 39 [See Eqs. (24)–(26)]. It is certainly valid at least at low temperatures, thus providing a justification for the discrete theoretical model assumed for the polaron state (see Fig. 2) which is in accordance with the CC diagram in Fig. 1 based entirely on experimental data. A confirmation of the adopted model can be seen in Sec. IV through the comparison between the theoretical rate equation used and the experimental data on the F^* ionization rate.
[41]T. Timusk, J. Phys. Chem. Solids 26, 849 (1965).
[42]L. F. Mollenauer, S. Pan, and A. Winnacker, Phys. Rev. Lett. 26, 1643 (1971).
[43]R. F. Wood and U. Öpik, Phys. Rev. 179, 772 (1969); 179, 783 (1969).
[44]A. M. Stoneham, *Theory of Defects in Solids* (Clarendon, Oxford, 1975).
[45]P. Podini, Phys. Rev. 141, 572 (1966).
[46]F. C. Brown, in *Point Defects in Solids,* edited by J. H. Crawford and L. M. Slifkin (Plenum, New York, 1972), Vol. 1.
[47]S. I. Pekar, *Issledovaniya po Elektronnoi Teorii Kristallov* (GITTL, Moscow, 1951).
[48]R. S. Crandall, Phys. Rev. 138, A1242 (1965).
[49]L. D. Landau and E. M. Lifshits, *Kvantovaya Mekhanika,* 3rd ed. (Nauka, Moskow, 1974).